Estimation of regional water-saving potential using remotely sensed evapotranspiration data

Zhigong Peng[a,b], Baozhong Zhang[a,b,*], Yu Liu[a,b], Zhuping Sheng[c]

[a]*State Key Laboratory of Simulation and Regulation of Water Cycle in River Basin, China Institute of Water Resources and Hydropower Research, Beijing 100038, China, email: zhangbaozhong333@163.com (B. Zhang)*
[b]*National Center of Efficient Irrigation Engineering and Technology Research, Beijing 100048, China*
[c]*Texas A&M AgriLife Research Center at El Paso, El Paso, Texas 79927, The United States of America*

ABSTRACT

Estimation of regional water-saving potential is useful to develop the appropriate irrigation scheme and manage water resources. A new calculation method of water-saving potential for crops, based on the remotely sensed evapotranspiration (RS ET) data, is presented in this paper. The regional crop water production function was established based on RS ET and RS yield data. And the ET under the highest crop water use efficiency (WUE) was determined by its crop water production function. A regional crop ET quota was proposed by comparing crop water requirement and the ET under the highest crop WUE. The regional water-saving potential in agriculture was determined by selecting a regional crop ET quota as a standard. The results indicated that: (1) the ET quotas for winter wheat and summer maize were 417 and 313 mm, respectively; and (2) as far as the regional water-saving potential for crops is concerned, summer maize is the largest, at 11.77 million m^3, followed by winter wheat, at 0.73 million m^3; and (3) the water-saving management area and water-saving volumes for main crops among different towns in Daxing county were analyzed. Meanwhile, the major water-saving management towns for wheat and maize were determined. The study will help planners and managers gaining a better insight into water management and water uses of crops.

Keywords: Remote sensing; Evapotranspiration; Crop production; Water use efficiency; Water-saving potential

1. Introduction

The global food crisis was mainly caused by water resources shortage [1,2]. The limit of water resources utilization has been reached or broken in many areas of main grain production, including the North China Plain (NCP). The NCP is the largest region of agricultural production in China [3]. It covers about 18 million ha of farmlands (18.3% of the national total) and produces about 21.6% of the total grain yield in China [4]. Therefore, agricultural production in this region plays an important role in relation to food security and economic development in China [5]. With the rapid development of agriculture and industry along with prolonged drought, there are serious shortage of water resources and serious contradiction between supplies and demands of water resources [6,7]; which has great influence on the development of national economy, improvement of living conditions, and protection of ecological environment [8,9]. In the NCP, irrigation is required to maintain high and steady crop production. However, excessive use of groundwater for irrigation has caused the rapid decline of groundwater levels at an average rate of about 1 m year^{-1} [10]. Therefore, it is of great importance to estimate the regional water-saving potential in agriculture, reduce agricultural water consumption and restore the groundwater resources [11–13].

Up to now, however, no unified method is available for the calculation and valuation of water-saving potential in

* Corresponding author.

agriculture [14–16]. According to quantity of water savings, agriculture water-saving potential could be divided into two categories: (a) engineering water-saving potential, defined as the difference between the water withdrawal in the source region and the amount of water delivered to field, and (b) natural water-saving potential, defined as reductions in ineffective evapotranspiration (ET), such as soil evaporation, irrigation water evaporation in fields and irrigation system, namely the real water-saving quantity, the detail could be found in the study by Shen et al. [17]. Due to the difficulty to acquire large-scale ET data by using conventional methods, previous studies mainly focused on the engineering water-saving quantity [18–25]; that is, water loss from canal seepage, operation spills, and field drainage. However, the seepage, spill, and field drainage are not lost and could be reused at the downstream site or by eco-environment [26]. On the other hand, with technical innovations in the field of remote sensing (RS), RS images have such attributes as high spatial-temporal resolution, bidirectional reflectance multi-spectral and others. Therefore, monitoring large-scale ET with high accuracy by using RS technology is feasible, which overcomes the limitations of calculation of regional ET using conventional methods based on monitoring data of weather stations [27–35]. Different from the conventional method of engineering water-saving, the regional water-saving potential in agricultural irrigation was calculated based on RS ET data, in which the water-saving effects are evaluated as the reduction of the regional water consumption rather than the quantity of water withdrawn for irrigation. Therefore, the regional water-saving potential in agricultural irrigation based on RS ET data belongs to natural water-saving potential.

In this paper, the regional crop water production functions were derived based on the analysis of the relationship among ET, crop production and water use efficiency (WUE) by using GIS and RS techniques. A regional crop ET quota is determined by comparing the crop water requirements and the ET under the highest crop WUE. Then the regional water-saving potential in agricultural irrigation was evaluated using the selected regional crop ET quota. At the same time, the water-saving potential at pixel scale could be calculated, which has practical significance for crop water-saving management. Such a new calculation method

of agricultural water-saving potential based on RS ET data is a good complement to other calculation methods of agricultural water-saving potential.

2. Materials and methods

2.1. Materials

2.1.1. Study area

Daxing County, comprising of 14 towns and 2 farms, is located in the northeastern part of the NCP and north-central of the Haihe River basin (Fig. 1), between latitude of 39°26′ and 39°50′N, and longitude of 116°13′ and 116°43′E [36]. The elevation of the northwest is 50 m, while that of the southeast is 15 m, and the total study area covers 1,044 km². The study area soils in 1 m soil depth are silt loam formed by loess deposits, and continuous clay can be found in some areas. The winter wheat was planted by early October and harvested by mid-June in the next year, and the summer maize was planted immediately. The local climate is sub-humid, with mean annual precipitation of 490 mm, mean annual temperature of 12.1°C, annual accumulated temperature (>10°C) of 4,730°C, mean frost-free days of 185 d, and mean annual evaporation from a free water surface of 1,800 mm. The spatial-temporal distribution of precipitation is uneven, of which more than 70% of the total precipitation occur in the summer months (from June to September) [37].

2.1.2. Data used

The following datasets were used in this paper: (1) the monthly RS ET dataset of Daxing County with a 30 m-space resolution and for the period from October 2005 to December of the next year were used. (2) Land use dataset of Daxing County with a 30 m-space resolution were provided in Albers projection and an Arcshape data format. The Landsat TM and the field data were used to interpret land use maps by supervision classification and visual interpretation, two crops were identified, including winter wheat and summer maize (Fig. 2). The accuracy of 96% for land use data is validated by 114 sampling points of global positioning system. According to field observation, growth periods for
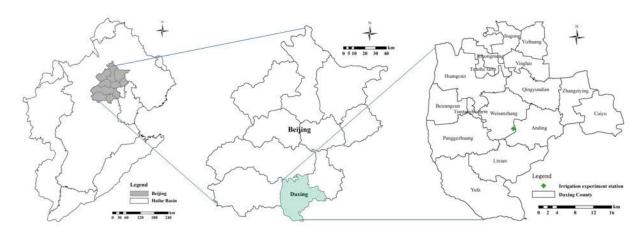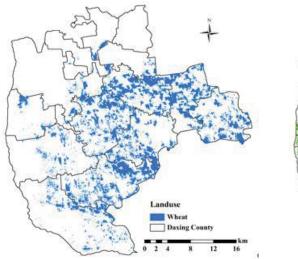
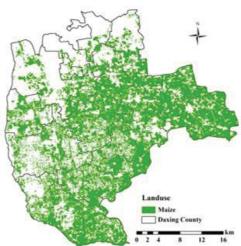

Fig. 1. Location of the study area.

Fig. 2. Land use of the study area.

the crops were identified as follows: from 8th October to 15th June for winter wheat and from 20th June to 30th September for summer maize. (3) In accordance with the crop growth season, the cumulative amount of the net primary productivity is the field dry matter in the agricultural area, which is calculated by using the Carnegie Ames Stanford Approach (CASA) Biosphere model [38]. The CASA model calculates the seasonal biomass increment of terrestrial crops based on ecological principles, satellite data, and surface data. The biomass increment is converted from the amount of photosynthetically active radiation absorbed by plants, depending on vegetation type and cover. This model has been verified in Yucheng, Shandong, Fengqiu, Henan, and Daxing (Beijing) [39]. (4) Meteorological data, such as air temperature, relative humidity, global and net radiation, and wind speed and direction at 2 m height, and precipitation were collected using an automatic weather station at the Irrigation Experiment Station of the China Institute of Water Resources and Hydropower Research (IWHR) at Daxing, Beijing region (39°37′ N, 116°26′ E and 40.1 m a.s.l.), which is located in central south of the study area in Daxing County (Fig. 1).

2.2. Methods

The crop WUE is calculated based on pixel data, such as RS ET and RS crop production. The reasonable ET quota should be located between the ET under the highest crop WUE and the theoretical crop water consumption under the highest crop production. Considering the water resources shortage in Daxing County, the crop ET quota could be determined based on the ET under the highest crop WUE. To avoid the inconsistency between the ET under the highest crop WUE and the results in the field experiment, the crop ET quota was corrected further by the crop water requirement. Then, regional water-saving potential in agriculture is calculated using crop ET quota as an evaluation criterion. The crop ET value of a pixel over the ET quota is considered as excessive water consumption. When the water consumption is lower than the crop ET quota, the crop ET data for a pixel

would be kept as is to account for other factors in determination of ET. Hence water-saving potential in agriculture based on RS ET can be achieved by controlling excessive water consumption for each pixel's ET data.

2.2.1. ETWatch model

ETWatch is a software originally designed to estimate ET based on remotely sensed land surface data as well as meteorological data, by integrating "Residue Approach" and Penman-Monteith (P-M) model [40,41]. First, the surface energy balance algorithm for land model, dealing with 30 m resolution RS data, and surface energy balance system model, dealing with 1 km resolution RS data are used to compute the ET. Due to cloud cover and satellite overpass interval, an adequate solution for the intermittent period based on the P–M model is then used to calculate daily ET data under all sky conditions. And the detail about ETWatch model can be obtained from the study by Wu et al. [40,41].

The ET validation of ETWatch using field measurements at the study area suggests that the average deviation in the agricultural area is about 10% [42].

2.2.2. Crop yield

The crop yield (Y) is defined as total dry matter of a specific crop, reflecting the economic output [43]. According to Howell's study [44], the harvest index (H_i) remains constant once the dry matter exceeded 8% of the maximum. Therefore, the H_i is set constant in many studies since the H_i becomes stable quickly. The linear relationship between the yield of the crop (i) and its dry matter is expressed in the following equation [3]:

$$Y_i = H_i \times \sum_{ts}^{te} DM \qquad (1)$$

where i is the crop type, DM is the incremental of the dry matter (kg hm^{-2}), H_i is the harvest index of the crop i, defined

as the ratio of yield and the ground dry matter [43]; 'ts' is the sowing time of the crop, and 'te' is the harvest time of the crop. The harvest index of food crops in China varies between 0.35 and 0.45. In the Hai Basin wheat and maize are the main crops based on the crop phonological calendar, the period from October to September of the following year is the growing season. The empirical coefficients of 0.361 for winter wheat and 0.433 for summer maize are used as the annual harvest index in this study. The dry matter and crop yield at the study area have been verified and analyzed in detail in previous studies [39,43].

2.2.3. Crop WUE

Crop WUE is defined as the crop yield produced for each unit of water consumed. The WUE is a comprehensive index to assess the performance of agricultural production and the rationality of agriculture water use [45–47]. It is defined as follows:

$$WUE_{sci} = Y_{sci}/ET_{sci} / 10 \tag{2}$$

where WUE_{sci} is i^{th} pixel's crop WUE in kg m^{-3}, Y_{sci} is i^{th} pixel's crop yield in kg hm^{-2} and ET_{sci} is i^{th} pixel's crop ET in mm, and 10 is the unit conversion coefficient.

2.2.4. Crop ET quota

With a 30 m space resolution of the RS ET dataset, there were thousands of pixels for one crop in the study area. If the crop water production function was established based on every pixel, data points would be too discrete to allow high-efficiency regression analysis. Considering the distribution of the RS ET dataset, the pixel value of RS ET was classified by an interval of 20 mm. As a result, the RS ET data of some crops could be divided into ranges, such as 60–80 mm, …, 460–480 mm, …, and so on. The average values of the classified RS ET were then calculated by using GIS techniques such as the tools of Reclassify and Zonal Statistics. The average values of crop WUE and crop yield were also calculated by using the classified RS ET. The relationship among RS ET, RS crop yield and crop WUE can be analyzed in the similar method. Based on the results from the crop water consumption experiments in the field, the relationship between crop WUE and water consumption is determined as a quadratic function [48]. The crop ET quota is calculated by Eq. (5), where the crop ET quota is further corrected by the crop water requirement. The formula for the ET quota is listed as follows:

$$WUE_{rc} = aET_{rc}^2 + bET_{rc} + c \tag{3}$$

$$ET_c = K_c \times ET_0 \tag{4}$$

$$ET_q = \begin{cases} -\dfrac{b}{2a} & \left(-\dfrac{b}{2a} \le ET_c\right) \\ ET_c & \left(ET_c < -\dfrac{b}{2a}\right) \end{cases} \tag{5}$$

where WUE_{rc} is the average value of crop WUE classified in kg m^{-3}, ET_{rc} is the average value of RS ET classified in mm, a and b are coefficients of the quadratic parabola, ET_c is crop water requirement in mm, ET_0 is the reference crop ET in mm, K_c is the crop coefficient and ET_q is the crop ET quota in mm. Here, the reference ET is calculated by using the FAO 56 Penman-Monteith's equation, and the crop coefficient is calculated by using the FAO 56 single-crop coefficient approach [49–53].

2.2.5. Water-saving potential in irrigated agriculture

The following formula was proposed to estimate water-saving potential (WSP) using ET quota:

$$WSP = \sum_{i=1}^{n} 0.9 \times WSP_{sci} \tag{6}$$

$$WSP_{sci} = ET_{sci} - ET_{adci} \tag{7}$$

$$ET_{adci} = \begin{cases} ET_{sci} & \left(ET_{sci} \le ET_q\right) \\ ET_q & \left(ET_{sci} > ET_q\right) \end{cases} \tag{8}$$

where WSP is the water-saving potential for some crop in m^3, WSP_{sci} is the ith pixel's water-saving potential in mm, ET_{sci} is the ith pixel's ET in mm, ET_{adci} is the adjusted ET for i^{th} pixel in mm and n is the number of pixels for the crops in the study area, and 0.9 is the unit conversion coefficient under 30 m space resolution pixel.

3. Results and discussion

3.1. WUE and regional ET quota

As shown in Fig. 3, the winter wheat yield increases proportionally, almost linearly, with the ET until it reaches its peak and decreases afterwards. Up to an ET value of 573 mm, the yield of winter wheat increases slowly with ET, but then declined when the ET continues to increase [54]. Before the crop ET reaches a threshold, winter wheat WUE increased with an increase in the ET.

Once the ET reaches its threshold ET, winter wheat WUE then declined as the ET increase further. Based on the relationship between WUE and ET for winter wheat, the crop water production function for winter wheat simulated by the quadratic parabola-fitting equation Eq. (9) is derived as follows:

$$WUE_{rc} = -0.00000814ET_{rc}^2 + 0.00679ET_{rc} - 0.102 \quad \left(R^2 = 0.782\right) \tag{9}$$

Based on the crop water production function for winter wheat, the threshold ET was determined as 417 mm, and its WUE was 1.31 kg m^{-3}. Similarly, based on the relationship between crop yield and ET for winter wheat, the crop yield was determined as 5,649 kg hm^{-2} when its ET reaches the threshold of 417 mm.

As shown in Fig. 4, summer maize yield increases proportionally, almost linearly, with an increase in ET. When
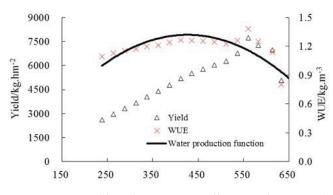
Fig. 3. Crop yield and water use efficiency change with evapotranspiration for winter wheat.
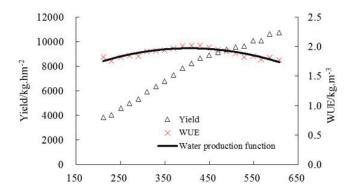

Fig. 4. Crop yield and water use efficiency change with ET for summer maize.

the ET of summer maize goes over 400 mm, the wheat yield increases at a lower rate. The relationship between WUE and ET for summer maize is similar to that for winter wheat [55]. The WUE of summer maize increases with an increase of the ET until it reaches its peak and decreases afterward. The crop water production function for summer maize simulated by the quadratic equation Eq. (10) was obtained with a very high *R*-squared value (0.821).

$$WUE_{rc} = -0.00000575ET_{rc}^2 + 0.00466ET_{rc} + 1.027 \ \left(R^2 = 0.821\right) \quad (10)$$

Based on the crop water production function for summer maize, the threshold ET was determined at 405 mm, and its WUE was 2.05 kg m^{-3}. The corresponding yield was 7,984 kg hm^{-2} at the threshold ET of 405 mm.

The average crop water requirements of winter wheat and summer maize were calculated as 434 and 313 mm, respectively. In this paper we choose the high yield and low ET at the largest crop WUE as evaluation criteria. The ET quota for winter wheat and summer maize were then determined as 417 and 313 mm, respectively.

3.2. Frequency distribution histogram of the ET, yield, and WUE of winter wheat and summer maize

Based on the mean values and variations of RS data, the distribution ratios of the ET, crop yield, and WUE for some crops were calculated using the NORMDIST function,

which calculates the cumulative distribution function of the standard normal distribution. As a result, the normal distributions of their RS data were assessed. The frequency distribution histograms of the winter wheat ET, its yield and its WUE are shown in Fig. 5. The winter wheat ET mainly ranges from 200 to 560 mm with an average of 328 mm and a variation of 80 mm. Winter wheat yield mainly ranges from 800 to 10,400 kg hm^{-2} with an average of 3,930 kg hm^{-2} and a variation of 2,003 kg hm^{-2}. The winter wheat WUE mainly ranges from 0.80 to 2.60 kg m^{-3} with an average of 1.18 kg m^{-3} and a variation of 0.55 kg m^{-3}. Based on the water production function of winter wheat and the relationship between the ET and RS crop yield, its yield and WUE were determined as 5,649 kg hm^{-2} and 1.31 kg m^{-3}, respectively, when the ET quota of winter wheat reached the threshold of 417 mm. Based on the NORMDIST function of RS data for winter wheat as shown in Fig. 5, the frequency ranges of the winter wheat ET quota, its yield and WUE were primarily located from 27% to 92%, 36% to 89%, and 24% to 87%, respectively. The frequency of ET, yield, and WUE was 89%, 85%, and 84%, respectively, when the ET quota of winter wheat reaches 417 mm. Therefore, the ET quota of 417 mm for winter wheat is a reasonable representation.

As shown in Fig. 6, the summer maize ET mainly ranges from 160 to 520 mm with an average of 302 mm and a variation of 68 mm. The summer maize yield mainly ranges from 800 to 10,000 kg hm^{-2} with an average of 5,751 kg hm^{-2} and a variation of 1,710 kg hm^{-2}. The summer maize WUE mainly ranges from 1.20 to 3.00 kg m^{-3} with an average of 1.88 kg m^{-3} and a variation of 0.26 kg m^{-3}. Based on the water production function of summer maize and the relationship between the ET and RS yield, its yield and WUE were determined as 5,999 kg hm^{-2} and 1.91 kg m^{-3}, respectively, when the ET quota of summer maize reached its threshold of 313 mm. Based on the NORMDIST function of the normal distribution of RS data for summer maize, the frequency ranges of the summer maize ET quota, its yield and its WUE were primarily located from 38% to 62%, 61% to 80%, and 36% to 87%, respectively. The frequency of ET, yield, and WUE were 58%, 61%, and 52%, respectively, when the ET quota of summer maize reached the threshold of 313 mm. Therefore, the ET quota of 313 mm of summer maize is a reasonable representation.

3.3. Crop yield frequency distribution under the ET quota neighborhood

There are two principles in the determination of ET quota and its yield neighborhood. One is no difference of pixels' value in the range of neighborhood, and the other is enough pixels for representativeness. When the interval of 10 mm was selected to determine the neighborhood of ET quota, there are about 5,000 pixels for winter wheat and 34,000 pixels for summer maize, respectively. The yield frequency distribution histograms of winter wheat under ET quota neighborhood are shown in Fig. 7(a). The neighborhood of winter wheat ET quota of 417 mm was in 410–420 mm. The frequency distribution of winter wheat yield in the neighborhood of ET quota mainly varied between 4,000 and 7,000 kg hm^{-2}, which accounted for about 74% of winter wheat yield in the neighborhood based on the NORMDIST
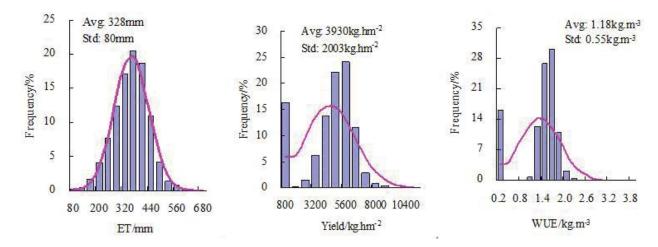
Fig. 5. Frequency distribution histogram of winter wheat ET, crop yield and water use efficiency.
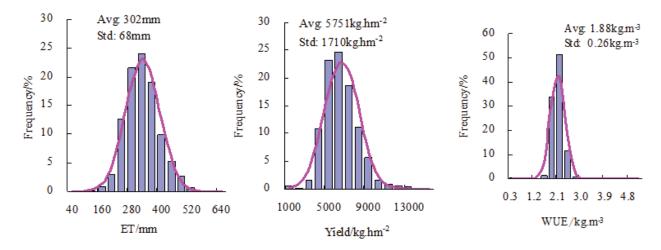

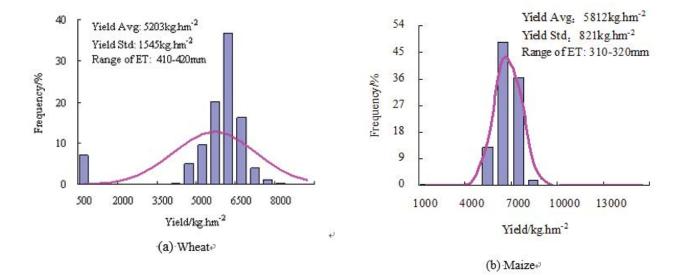Fig. 6. Frequency distribution histogram of summer maize ET, crop yield, and water use efficiency.

Fig. 7. Histogram of the crop yield under the ET quota neighborhood.

function. Approximately 52.29% of winter wheat pixel's yield in the neighborhood of ET quota was lower than the winter wheat yield of 5,649 kg hm^{-2} under ET quota. If the ET of winter wheat remained unchanged, winter wheat yield could be increased by adopting agricultural management practices such as balanced fertilization techniques and others.

As shown in Fig. 7(b), the neighborhood of summer maize ET quota 313 mm ranges from 310 to 320 mm, and the frequency distribution of summer maize yield in the neighborhood of ET quota ranges from 3,500 to 6,500 kg hm^{-2}, which accounted for about 99% of that in the neighborhood of ET quota. It was estimated that 61.44% of summer maize pixel's yield in the neighborhood of ET quota was lower than the summer maize yield of 6,000 kg hm^{-2} under ET quota. If the ET of summer maize remained unchanged, summer maize yield could be increased by adopting some agricultural management practices. In sum, the calculated crop ET quota is feasible, and the crop yield under ET quota could be increased by implementing some agricultural management practices.

3.4. ET frequency distribution under the ET quota yield neighborhood

When the interval of 100 kg hm^{-2} was selected to determine the neighborhood of ET quota yield, there are over 3,000 pixels for winter wheat and 12,000 pixels for summer maize, respectively. The ET frequency distribution histograms of winter wheat and summer maize under ET quota yield neighborhood are shown in Fig. 8. The neighborhood of winter wheat ET quota yield of 5,649 kg hm^{-2} ranges from 5,600 to 5,700 kg hm^{-2}, and the frequency distribution of the ET under the winter wheat ET quota yield neighborhood was normally distributed mainly from 360 to 450 mm, which accounted for 93.67%. It was estimated that, approximately, 21.74% of winter wheat pixel's ET in the neighborhood of winter wheat ET quota yield were higher than the winter wheat ET quota of 417 mm. If winter wheat yield remained unchanged, the winter wheat ET could be decreased by

using water-saving measures such as optimal irrigation scheduling. The neighborhood of the summer maize ET quota yield of 6,000 kg hm^{-2} was from 5,950 to 6,050 kg hm^{-2}, and the frequency distribution of ET under summer maize ET quota yield neighborhood was mainly from 260 to 420 mm, which accounted for over 99%. It was estimated that approximately 50.93% of summer maize pixel's ET in the neighborhood of the summer maize ET quota yield were higher than the summer maize ET quota of 313 mm. According to water-saving concept, namely a reduction in crop water consumption without a reduction in crop yield, the winter wheat and summer maize ET quotas were validated, proving that the calculated crop ET quota was feasible. It was further concluded that calculated crop ET quota could be further compressed or reduced.
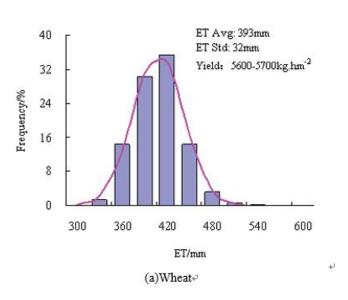
3.5. Crop water-saving potential

The ET quotas for winter and summer maize were determined as 417 and 313 mm, respectively, as shown in the previous section. The crop water-saving potential under ET quota management for these two crops was analyzed, and the results are shown in Table 1. Considering the crop planting area, summer maize covers the largest area, accounting for 50.57% of Daxing County area. Summer maize was followed by winter wheat, accounting for 15.35%. Once crop ET quota was determined, crop water-saving potential could be

Table 1
Water saving potential for main crops under ET quota management

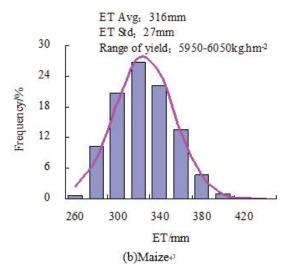| Items	Wheat	Maize
Planting area (km²)	160.23	527.79
Proportion of Daxing County (%)	15.35	50.57
ET quota (mm)	417.00	313.00
Water-saving volume (10⁶ m³)	0.73	11.77

Fig. 8. Histogram of the crop ET under the ET quota yield neighborhood.

acquired by adjusting the current pixels' ET value. Considering water-saving potential, summer maize would contribute the largest, with approximately 11.77 million m³, followed by winter wheat, with 0.73 million m³. The quantity of water-saving depends on two major factors: the crop planting area and the difference between the current average ET and the adjusted average ET. Therefore, we should target water-savings volume on wheat production because it grows in a dry season and depends on irrigation. However, it is difficult to control water consumption for maize production since that grows in a rainy season.

To demonstrate application of the new method, water-saving volumes for main crops among towns as well as water-saving management area within each town in Daxing county were analyzed. The results are shown in Table 2 and Fig. 9. Comparing water-saving volumes of wheat in the study area, we found that Qingyundian was the largest, with approximately 0.228×10^6 m³, followed by Jiugong, with 0.194×10^6 m³, then by Changziying with 0.130×10^6 m³, and the least by Tiantanghe farm, with no water-saving volume. In terms of water-saving volume for maize, Beizangcun was the largest, with approximately 1.843×10^6 m³, followed by

Table 2
Water-saving volumes for main crops within water-saving management areas among towns in Daxing county

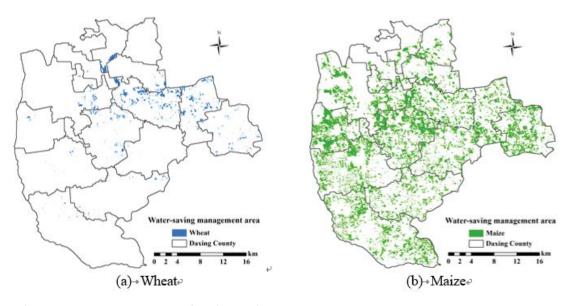| Towns and farms	ET quota management area (km²)		Water-saving volume (10^6 m³)	
	Wheat	Maize	Wheat	Maize
Yizhuang	0.000	4.424	0.000	0.393
Jiugong	1.579	3.059	0.194	0.234
Xihongmen	0.190	1.923	0.011	0.114
Huangcun	1.128	21.503	0.034	1.416
Yinghai	0.753	4.924	0.030	0.322
Tuanhe farm	0.150	1.715	0.013	0.095
Qingyundian	6.064	17.261	0.228	0.910
Changziying	3.524	12.773	0.130	0.524
Caiyu	1.229	19.931	0.027	0.914
Beizangcun	0.185	19.762	0.005	1.843
Weishanzhuang	1.815	27.401	0.043	1.337
Tiantanghe farm	0.003	1.355	0.000	0.069
Anding	0.083	14.937	0.002	0.703
Panggezhuang	0.185	22.271	0.003	1.293
Lixian	0.362	15.007	0.007	0.481
Yufa	0.179	30.235	0.004	1.121
Total	17.428	218.481	0.730	11.770

Fig. 9. Maps of water-saving management area for wheat and maize in Daxing County.

Huangcun, with 1.416×10^6 m^3, then by Weishanzhuang with 1.337×10^6 m^3, and the least by Tiantanghe farm, with 0.069×10^6 m^3.

The water-saving management area for winter wheat was 17.428 km^2, which accounted for 10.88% of winter wheat planting area. In terms of water-saving management area for winter wheat, Qingyundian was the largest, with approximately 6.064 km^2, followed by Changziying, with 3.524 km^2, then by Weishanzhuang, with 1.815 km^2, and the least by Tiantanghe farm, with about 0.003 km^2. The water-saving management area for maize was 214.481 km^2, accounting for 41.40% of the maize planting area. In comparison of the water-saving management area for maize in the study area, Yufa was the largest, with approximately 30.235 km^2, followed by Weishanzhuang, with 27.401 km^2, then by Panggezhuang, with 22.271 km^2, and the least by Tiantanghe farm, with about 1.355 km^2.

Based on a comprehensive consideration of water-saving volume for main crops within the water-saving management area among towns, the major towns for winter wheat were Qingyundian, Changziying, and Jiugong; the major towns for maize were Beizangcun, Huangcun, and Weishanzhuang. For the water-saving management area, measures could be taken to reduce the water consumption, for example, the optimal irrigation schedule for winter wheat; the dry-land farming for summer maize.

4. Conclusions

The relationship among RS ET, RS crop yield and crop WUE was analyzed, a quadratic model between the RS ET and crop WUE was identified by using statistical regression, and the ET quota of main crops was determined. Basis of this, a new calculation of water-saving potential for crops is presented. The new method presented in this paper accounts for natural water-saving potential by assessing the water saving potential at a pixel scale, complementing other methods. The conclusions were drawn as follows:

- The rational ET quotas are the base for calculating the crop water-saving potential. The ET quotas of winter wheat and summer maize were 417 and 313 mm, respectively. The rationality of the calculated crop ET quotas was validated by the frequency distribution histogram of RS ET, RS crop yield and crop WUE and water-saving concept, namely, by reducing crop water consumption without a reduction in crop yield and by increasing crop yield without an increase in crop water consumption.
- Regional water-saving potential was calculated by comparing the current ET values with the adjusted pixel's ET values using the selected crop ET quota as evaluation criteria. It was concluded that summer maize has the largest potential, at 11.77 million m^3, followed by winter wheat, at 0.73 million m^3.
- Furthermore, for winter wheat and summer maize, the towns of water-saving management were selected. Therefore, water-saving potential and water-saving management area for main crops could be calculated by the method, which is benefit to regional agriculture water management.

References

[1] J.S. Wallace, Increasing agricultural water use efficiency to meet future food production, Agric. Ecosyst. Environ., 82 (2000) 105–119.
[2] Y.B. Wang, P.T. Wu, B.A. Engel, S.K. Sun, Application of water footprint combined with a unified virtual crop pattern to evaluate crop water productivity in grain production in China, Sci. Total Environ., 497–498 (2014) 1–9.
[3] Z. Yan, C. Gao, Y. Ren, R. Zong, Y. Ma, Q. Li, Effects of pre-sowing irrigation and straw mulching on the grain yield and water use efficiency of summer maize in the North China Plain, Agric. Water Manage., 186 (2017) 21–28.
[4] H.Y. Sun, Y.J. Shen, Q. Yu, G.N. Flerchinger, Y. Zhang, C. Liu, X. Zhang, Effect of precipitation change on water balance and WUE of the winter wheat-summer maize rotation in the North China Plain, Agric. Water Manage., 97 (2010) 1139–1145.
[5] X. Liu, Y. Li, W. Hao, Tread and causes of water requirement of main crops in North China in recent 50 years, Trans. Chin. Soc. Agric. Eng., 21 (2005) 155–159.
[6] Z.W. Song, H.L. Zhang, R.L. Snyder, F.E. Anderson, F. Chen, Distribution and trends in reference Evapotranspiration in the North China Plain, J. Irrig. Drain. Eng., 136 (2010) 240–247.
[7] X. Yang, Y. Chen, S. Racenka, W. Gao, L. Ma, G. Wang, P. Yan, P. Sui, T. Steenhuis, Effect of diversified crop rotations on groundwater levels and crop water productivity in the North China Plain, J. Hydrol., 522 (2015) 428–438.
[8] Y. Yang, Y. Yang, J.P. Moiwo, Y. Hu, Estimation of irrigation requirement for sustainable water resources reallocation in North China, Agric. Water Manage., 97 (2010) 1711–1721.
[9] R. Zhang, Groundwater hydrograph patterns in North China Plain during 1982–1986 interpreted using principal component analysis, Adv. Mater. Res., 356–360 (2012) 2320–2324.
[10] C. Chen, E. Wang, Q. Yu, Modeling wheat and maize productivity as affected by climate variation and irrigation supply in North China Plain, Agron. J., 3 (2010) 1037–1049.
[11] S. Lopez, B. Lima, M. Belen Aguero, M. Liza Lopez, M. Hadad, J. Zygadlo, D. Caballero, R. Stariolo, E. Suero, G. Egly Feresin, A. Tapia, Chemical composition, antibacterial and repellent activities of *Azorella trifurcata*, *Senecio pogonias*, and *Senecio oreophyton* essential oils, Arabian J. Chem., 11 (2018) 181–187.
[12] M.M. Morones Esquivel, J.C. Pantoja Espinoza, J.B. Proal Najera, I. Chairez Hernandez, J.N. Gurrola Reyes, M. Avila Santos, Use of a plate reactor (tio$_2$/glass) for the degradation of 2,5-diclorofenol by solar photocatalisis, Revista Internacional De Contaminacion Ambiental, 33 (2017) 605–616.
[13] A. Tomporowski, J. Flizikowski, M. Opielak, R. Kasner, W. Kruszelnicka, Assessment of energy use and elimination of Co2 emissions in the life cycle of an offshore wind power plant farm, Polish Marit. Res., 24 (2017) 93–101.
[14] W. Gao, W. Wang, New isolated toughness condition for fractional (*g, f, n*) - critical graph, Colloquium Mathematicum, 147 (2017) 55–65.
[15] Z. Liu, Economic analysis of energy production from coal/biomass upgrading; Part 1: hydrogen production, Energy Sources, Part B: Econ. Plann. Policy, 13 (2018) 132–136.
[16] W. Peng, A. Maleki, M.A. Rosen, P. Azarikhah, Optimization of a hybrid system for solar-wind-based water desalination by

reverse osmosis: comparison of approaches, Desalination, 442 (2018) 16–31.

[17] Z.R. Shen, L. Wang, F.L. Yu, B. Liu, New Concept of Water Saving—Study and Application of Real Water Saving, China Water Power Press, Beijing, China, 2000.

[18] A. Blanke, S. Rozelle, B. Lohmar, J. Wang, J. Huang, Water saving technology and saving water in China, Agric. Water Manage., 87 (2007) 139–150.

[19] K. Damerau, A.G. Patt, O. Vliet, Water saving potentials and possible trade-offs for future food and energy supply, Global Environ. Change, 39 (2016) 15–25.

[20] A.W. Duan, N.Q. Xin, L.X. Wang, Exploitation of water-saving potential in irrigation agriculture in northwest China, Rev. China Agric. Sci. Technol., 4 (2002) 50–55.

[21] Q.Z. Gao, H.L. Du, R.P. Zu, The balance between supply and demand of water resources and the water-saving potential for agriculture in the Hexi Corridor, Chin. Geogr. Sci., 12 (2002) 23–29.

[22] X. Jin, Q. Zuo, W. Ma, S. Li, J. Shi, Y. Tao, Y. Zhang, Y. Liu, X. Liu, S. Lin, A. Ben-Gal, Water consumption and water-saving characteristics of a ground cover rice production system, J. Hydrol., 540 (2016) 220–231.

[23] A. Kalbusch, E. Ghisi, Comparative life-cycle assessment of ordinary and water-saving taps, J. Cleaner Prod., 112 (2016) 4585–4593.

[24] Y.S. Pei, J.P. Zhang, Y. Zhao, Water saving potential in irrigation area of Ningxia Autonomous Region, J. Hydraul. Eng., 38 (2007) 239–243.

[25] M. Wang, G. Shao, J. Meng, C. Chen, D. Huang, Variable fuzzy assessment of water use efficiency and benefits in irrigation district, Water Sci. Eng., 8 (2005) 205–210.

[26] Y.G. Li, Real water-saving based on ET management, Hebei. Water Resour., 2 (2007) 26–26, 28.

[27] H. Ahmadzadeh, S. Morid, M. Delavar, R. Srinivasan, Using the SWAT model to assess the impacts of changing irrigation from surface to pressurized systems on water productivity and water saving in the Zarrineh Rud catchment, Agric. Water Manage., 175 (2016) 15–28.

[28] Y. Chen, X. Li, P. Shi, Estimation of regional evapotranspiration over Northwest China using remote sensing, J. Geog. Sci., 11 (2008) 140–148.

[29] Y.B. He, Z.B. Su, J. Li, S.L. Wang, Estimation of surface energy flux using surface energy balance system (SEBS) in the Yellow-Huaihe-Haihe river regions, China, Plateau Meteorol., 25 (2006) 1092–1100.

[30] Z.Q. Pan, G.H. Liu, C.G. Zhou, Dynamic analysis of evapotranspiration based on remote sensing in Yellow River Delta, J. Geog. Sci., 13 (2008) 408–415.

[31] H.G. Prasanna, L.C. Jose, D.C. Paul, R.E. Steve, A.H. Terry, A.T. Judy, ET mapping for agricultural water management: present status and challenges, Irrig. Sci., 26 (2008) 223–237.

[32] Z. Samani, A.S. Bawazir, M. Bleiweiss, R. Skaggs, J. Longworth, V.D. Tran, A. Pinon, Using remote sensing to evaluate the spatial variability of evapotranspiration and crop coefficient in the lower Rio Grande Valley, New Mexico, Irrig. Sci., 28 (2009) 93–100.

[33] C. Santos, I.J. Lorite, M. Tasumi, R.G. Allen, E. Fereres, Integrating satellite-based evapotranspiration with simulation models for irrigation management at the scheme level, Irrig. Sci., 26 (2008) 277–288.

[34] M. Tasimi, R. Trezza, R.G. Allen, J.L. Wright, Operational aspects of satellite-based energy balance models for irrigated crops in the semi-arid U.S., Irrig. Drain. Syst., 19 (2005) 355–376.

[35] H. Wonsook, H.G. Prasanna, A.H. Terry, A review of downscaling methods for remote sensing-based irrigation management: Part I, Irrig. Sci., 31 (2013) 831–850.

[36] P. Meng, J. Hao, W. Guo, M. Hou, L. Qin, A case study on the application of location models for small town development of Daxing district Beijing, J. Chin. Agric. Univ., 3 (2004) 88-92.

[37] Beijing Daxing Bureau of Water Resources, Integrated Planning of Water Resources in Daxing Beijing, Beijing, October 2004.

[38] C.B. Field, J.T. Randerson, C.M. Malmstrom, Global net primary production: combining ecology and remote sensing, Remote Sens. Environ., 51 (1995) 74–88.

[39] X. Du, B.F. Wu, J.H. Meng, Q.Z. Li, F.F. Zhang, A method to assess land productivity in Huang-Huai-Hai region using remote sensing, ICMT Proceeding, Ningbo, China, 2010.

[40] B. Wu, J. Xiong, N. Yan, L. Yang, X. Du, ETWatch for monitoring regional evapotranspiration with remote sensing, Adv. Water Sci., 19 (2008) 671–678.

[41] B. Wu, J. Xiong, N. Yan, ETWatch: models and methods, J. Remote Sens., 15 (2010) 224–230.

[42] B. Wu, N. Yan, J. Xiong, W.G.M. Bastiaanssen, W. Zhu, A. Stein, Validation of ETWatch using field measurements at diverse landscapes: a case study in Hai Basin of China, J. Hydrol., 436–437 (2012) 67–80.

[43] N. Yan, B. Wu, X. Du, Estimation of agricultural water productivity an application, J. Remote Sens., 15 (2011) 298–304.

[44] T.A. Howell, Relationship between crop production and Transpiration, evapotranspiration and irrigation, Irrig. Agric. Crop Agron. Monogr., 30 (2009) 292–427.

[45] E.I. Henry, F.M. Henry, K. Andrem, A.S. Baanda, Crop water productivity of an irrigated maize crop in Mkoji Sub-catchment of the Great Ruaha River Basin, Tanzania, Agric. Water Manage., 85 (2006) 141–150.

[46] A. Keller, J. Keller, D. Seckler, Integrated water resource systems: theory and policy implications, Research Report 3, International Water Management Institute, Colombo, Sri Lanka, 1996.

[47] J.Z. Sander, G.M.B. Wim, Review of measured crop water productivity values for irrigated wheat, rice, cotton and maize, Agric. Water Manage., 69 (2004) 115–133.

[48] Y.Q. Zhang, E. Kendy, Q. Yu, C.M. Liu, Y.J. Shen, H.Y. Sun, Effect of soil water deficit on evapotranspiration, crop yield, and water use efficiency in the North China Plain, Agric. Water Manage., 64 (2004) 107–122.

[49] R.G. Allen, L.S. Pereira, D. Raes, M. Smith, Crop evapotranspiration guidelines for computing crop water requirements. FAO Irrigation and Drainage Paper, 1998, p. 56.

[50] C.M. Donald, J. Hamblin, The biological yield and harvest index of cereals as agronomic and plant breeding criteria, Adv. Agron., 28 (1976) 361–405.

[51] A.H. Kori, M.A. Jakhrani, S.A. Mahesar, G.Q. Shar, M.S. Jagirani, A.R. Shar, O.M. Sahito, Risk assessment of arsenic in ground water of Larkana city, Geol. Ecol. Landscapes, 2 (2018) 8–14.

[52] H. Amin, B.A. Arain, M.S. Abbasi, T.M. Jahangir, F. Amin, Comparative study of Zn-phytoextraction potential in guar (*Cyamopsis tetragonoloba* L.) and sesame (*Sesamum indicum* L.): tolerance and accumulation, Geol. Ecol. Landscapes, 2 (2018) 29–38.

[53] T.H.T. Ismail, N.A.F. Adnan, M.A.A. Samah, Study on accumulation of Fe, Pb, Zn, Ni and Cd in Nerita lineata and Thais bitubercularis obtained from Tanjung Harapan and Teluk Kemang, Malaysia. J. CleanWAS, 1 (2017) 06–16.

[54] A.I. Gogoba, H.M.M. Peralta, H. Basri, M.M. Nmaya, Inhibitory effect of pigment extract from scenedesmus sp. on food spiked with foodborne staphylococcus aureus, J. CleanWAS, 1 (2017) 23–25.

[55] N.S. Zafisah, W.L. Ang, A.W. Mohammad, Cake filtration for suspended solids removal in digestate from anaerobic digested palm oil mill effluent (POME), Water Conserv. Manage., 2 (2018) 5–9.